

Thermophysical Properties of Five Acetate-Based Ionic Liquids

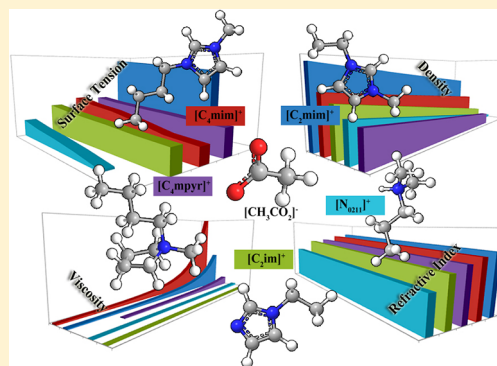
Hugo F. D. Almeida,[†] Helena Passos,[†] José A. Lopes-da-Silva,[‡] Ana M. Fernandes,[‡] Mara G. Freire,^{*,†} and João A. P. Coutinho[†]

[†]Departamento de Química, CICECO, Universidade de Aveiro, 3810-193 Aveiro, Portugal

[‡]QOPNA Unit, Departamento de Química, Universidade de Aveiro, 3810-193 Aveiro, Portugal

Supporting Information

ABSTRACT: Ionic liquids (ILs) with improved hydrogen-bonding acceptor abilities, such as acetate-based compounds, have shown great potential for CO₂ capture and biomass dissolution. In this context, the knowledge of the thermophysical properties of acetate-based fluids is essential for the design and scale-up of related processes. However, at this stage, acetate-based ILs are still poorly characterized. In this work, four thermophysical properties, specifically, density, viscosity, refractive index, and surface tension, were determined for five acetate-based ILs. Both protic and aprotic ILs were investigated, namely, *N,N*-dimethyl-*N*-ethylammonium acetate, 1-ethylimidazolium acetate, 1-ethyl-3-methylimidazolium acetate, 1-butyl-3-methylimidazolium acetate, and 1-butyl-1-methylpyrrolidinium acetate. From the temperature dependence of the measured properties, additional properties, such as the isobaric thermal expansion coefficient, the surface entropy and enthalpy, and the critical temperature, were further estimated.



INTRODUCTION

During the past decade research has emerged in various areas involving ionic liquids (ILs), and their potential applications are nowadays widespread. Ionic liquids are a group of molten salts normally composed of inorganic or organic anions, and relatively large organic cations, which do not easily form an ordered crystal and, therefore, they remain liquid at or near room temperature.^{1–3}

Recently, certain classes of ILs with improved hydrogen-bonding acceptor capability, such as acetate-based fluids, have shown to be promising solvents for CO₂ capture^{4–7} and cellulose and/or biomass dissolution.^{8–11} Acetate-based fluids are able to strongly coordinate with CO₂ and hydrogen bond donor groups, such as –OH groups, and favorable results have thus been published. Moreover, acetate-based ILs present low toxicity, low corrosiveness, and favorable biodegradability.¹² Despite their undeniable interest, the thermophysical properties of acetate-based fluids are still poorly characterized. In a previous work we have determined the densities and viscosities of a series of imidazolium-based ILs which have shown potential for the dissolution of biomass.¹³ Fendt et al.¹⁴ presented the viscosities of acetate-based ILs and some of their mixtures with water and organic solvents. Qian et al.¹⁵ explored the densities and viscosities of the protic IL 1-methylimidazolium acetate and its binary mixtures with alcohols. Additional scarce reports have addressed the measurements of densities,^{16–18} viscosities,¹⁹ refractive index,^{16,20} and surface tension¹⁸ of aprotic acetate-based ILs.

In this work, the thermophysical properties of acetate-based ILs, specifically density, viscosity, refractive index, and surface

tension, were measured as a function of temperature. The ILs are formed by the common anion acetate, combined either with protic (*N,N*-dimethyl-*N*-ethylammonium and 1-ethylimidazolium) or aprotic cations (1-ethyl-3-methylimidazolium, 1-butyl-3-methylimidazolium and 1-butyl-1-methylpyrrolidinium). Additional properties, such as the isobaric thermal expansion coefficient, the surface thermodynamics properties, and critical temperature of all ILs studied were also estimated. For the density and refractive index experimental data, further comparisons with the predictions by the Gardas and Coutinho group contribution methods^{21,22} were carried out, and new group parameters for chemical groups not previously available are proposed.

EXPERIMENTAL SECTION

Materials. Five ILs were studied in this work, namely, *N,N*-dimethyl-*N*-ethylammonium acetate [N₀₁₁₂][CH₃CO₂] (purity 98 wt %), 1-ethylimidazolium acetate [C₂im][CH₃CO₂] (purity > 97 wt %), 1-ethyl-3-methylimidazolium acetate [C₂mim][CH₃CO₂] (purity 99 wt %, CAS Registry No. 143314-17-4), 1-butyl-3-methylimidazolium acetate [C₄mim][CH₃CO₂] (purity > 98 wt %, CAS Registry No. 284049-75-8), and 1-butyl-1-methylpyrrolidinium acetate [C₄mpyr][CH₃CO₂] (purity 97 wt %). The ionic structures of the investigated ILs are depicted in Figure 1. All of the compounds were acquired at Iolitec.

Received: May 29, 2012

Accepted: September 27, 2012

Published: October 9, 2012

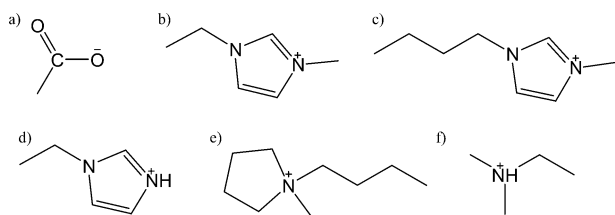


Figure 1. Ionic structures of (a) acetate ($[\text{CH}_3\text{CO}_2]^-$); (b) 1-ethyl-3-methylimidazolium ($[\text{C}_2\text{mim}]^+$); (c) 1-butyl-3-methylimidazolium ($[\text{C}_4\text{mim}]^+$); (d) 1-ethylimidazolium ($[\text{C}_2\text{im}]^+$); (e) 1-butyl-1-methylpyrrolidinium ($[\text{C}_4\text{mpyr}]^+$); (f) *N,N*-dimethyl-*N*-ethylammonium ($[\text{N}_{0112}]^+$).

To remove traces of water and volatile compounds for the aprotic ILs ($[\text{C}_2\text{mim}][\text{CH}_3\text{CO}_2]$, $[\text{C}_4\text{mim}][\text{CH}_3\text{CO}_2]$, and $[\text{C}_4\text{mpyr}][\text{CH}_3\text{CO}_2]$), individual samples of each fluid were dried at moderate temperature (≈ 313 K) and at high vacuum ($\approx 10^{-5}$ Pa) for a minimum period of 48 h under constant stirring. For the protic ILs ($[\text{N}_{0112}][\text{CH}_3\text{CO}_2]$ and $[\text{C}_2\text{im}][\text{CH}_3\text{CO}_2]$) samples were first distilled at room temperature, under constant stirring, and high vacuum for a period time of 12 h. This first step allowed the separation of the distilled IL from solid residues. After this prepurification step, individual samples of each protic fluid, the distillate fraction, were collected and further dried for 30 min, as described above, to remove the water traces and volatile compounds. After these purification procedures, the purity of all ILs samples was further checked by ^1H and ^{13}C NMR and is in accordance with the purities given by the supplier. The water content of each IL, after the drying step and immediately before the measurements of their thermophysical properties, was determined by Karl Fischer titration, making use of a Metrohm 831 Karl Fischer coulometer. Moreover, after the measurements on the thermophysical properties, the water content was also determined to ascertain on the water uptake by ILs during the experimental procedures. No significant differences were observed. The reagent used was Hydranal-Coulomat AG from Riedel-de Haën. The average water content of each IL is presented in Table 1.

Table 1. Water Content (Weight Fraction Percentages) in the Studied ILs

ionic liquid	water content/(wt %)
$[\text{C}_2\text{im}][\text{CH}_3\text{CO}_2]$	0.049
$[\text{C}_2\text{mim}][\text{CH}_3\text{CO}_2]$	0.046
$[\text{C}_4\text{mim}][\text{CH}_3\text{CO}_2]$	0.085
$[\text{C}_4\text{mpyr}][\text{CH}_3\text{CO}_2]$	0.070
$[\text{N}_{0211}][\text{CH}_3\text{CO}_2]$	0.056

EXPERIMENTAL PROCEDURE

Density and Viscosity. Density (ρ) and dynamic viscosity (η) measurements were carried out using an automated SVM 300 Anton Paar rotational Stabinger viscometer-densimeter in the temperature range from (283.15 to 363.15) K and at atmospheric pressure (≈ 0.1 MPa). Since the IL $[\text{C}_4\text{mpyr}][\text{CH}_3\text{CO}_2]$ is solid at room temperature, densities and viscosities were only determined above its melting temperature. The absolute uncertainty in density is ± 0.5 $\text{kg}\cdot\text{m}^{-3}$, and the relative uncertainty in dynamic viscosity is ± 0.35 %. The relative uncertainty in temperature is within ± 0.02 K. Further

details on the use of the same equipment for the determination of viscosities and densities of ILs can be found elsewhere.^{23–25}

Refractive Index. Measurements of refractive index (n_D) were performed at 589.3 nm using an automated Abbat 500 Anton Paar refractometer, able to measure both liquid and solid samples. Refractive index measurements were carried out in the temperature range from (283.15 to 353.15) K and at atmospheric pressure. The Abbat 500 Anton Paar refractometer uses reflected light to measure the refractive index, where the sample on the top of the measuring prism is irradiated from different angles by a light-emitting diode (LED). The maximum deviation in temperature is ± 0.01 K, and the maximum uncertainty in the refractive index measurements is $\pm 2\cdot 10^{-5}$.

Surface Tension. The surface tension of each compound was determined through the analysis of the shape of the pendant drop using a Dataphysics contact angle system OCA-20. Drop volumes of (14 ± 1) μL , depending on the IL, were obtained using a Hamilton DS 500/GT syringe with a Teflon coated needle. The needle is placed in a double-jacketed aluminum air chamber capable of maintaining the temperature within ± 0.1 K. The surface tension measurements were performed in the temperature range from (298 to 344) K and at atmospheric pressure. After reaching a specific temperature, the measurements were carried out after 30 min to guarantee the thermal equilibrium. Silica gel was kept inside the air chamber to avoid the adsorption of moisture. For the surface tension determination, at each temperature and for each IL, at least seven drops were formed and analyzed. For each drop, an average of 100 images was additionally captured. The analysis of the drop shape was performed with the software modules SCA 20. The density values for $[\text{C}_2\text{mim}][\text{CH}_3\text{CO}_2]$, required for the calculation of the surface tensions from the drop image data, were previously measured by us.¹³ The density data used for the remaining ILs were those determined in this work. To validate the equipment and methodology used, the surface tensions of ultrapure water, decane, and dodecane were also determined and agree with literature data.^{26–28} Further details on the equipment and its validity to measure surface tensions of ILs were previously reported.²⁹

RESULTS AND DISCUSSION

The thermal stability of ILs is a crucial factor regarding their possible applications. To ascertain on the thermal stability of the investigated acetate-based ILs, initial thermogravimetric analysis (TGA) assays were conducted. Details on the experimental procedure and results are provided in the Supporting Information (Figure S1). Protic acetate-based ILs began to lose weight below 320 K. Indeed, there is a continuous and slow loss of weight until 380 K for $[\text{N}_{0211}][\text{CH}_3\text{CO}_2]$ and until 410 K for $[\text{C}_2\text{im}][\text{CH}_3\text{CO}_2]$. This behavior is a direct result of the deprotonation of the cation with the further formation of the original base and acetic acid. Among the aprotic ILs, both $[\text{C}_2\text{mim}][\text{CH}_3\text{CO}_2]$ and $[\text{C}_4\text{mim}][\text{CH}_3\text{CO}_2]$ do not suffer significant weight loss until 470 K, while $[\text{C}_4\text{mpyr}][\text{CH}_3\text{CO}_2]$ shows to be less stable and starts to suffer degradation at circa 430 K. Nevertheless, it should be pointed out that to better establish the real thermal stability of the studied ILs, isothermal thermal analysis is further recommended.^{30,31}

Density. The new experimental density data are presented in Table 2. The densities for $[\text{C}_2\text{mim}][\text{CH}_3\text{CO}_2]$ were previously reported by us.¹³ Figure S2, provided in the

Table 2. Experimental Density Values, ρ , at Temperature T , for the Studied ILs at Pressure $p = 0.1$ MPa^a

T/K	$\rho/(\text{kg}\cdot\text{m}^{-3})$			
	$[\text{C}_2\text{im}][\text{CH}_3\text{CO}_2]$	$[\text{C}_4\text{mim}][\text{CH}_3\text{CO}_2]$	$[\text{C}_4\text{mpyr}][\text{CH}_3\text{CO}_2]$	$[\text{N}_{0122}][\text{CH}_3\text{CO}_2]$
283.15	1047.2	1062.2		1028.0
288.15	1042.9	1058.9		1024.0
293.15	1038.5	1055.5		1020.1
298.15	1034.2	1052.3	1021.2	1016.1
303.15	1029.9	1049.2	1018.1	1012.2
308.15	1025.6	1046.1	1015.1	1008.3
313.15	1021.3	1043.0	1012.1	1004.4
318.15	1017.0	1040.0	1009.2	1000.5
323.15	1012.7	1037.0	1006.2	996.8
328.15	1008.4	1034.0	1003.3	992.9
333.15	1004.1	1031.0	1000.4	989.0
338.15	999.8	1028.0	997.8	985.0
343.15	995.8	1025.0	994.9	981.1
348.15	991.5	1022.1	992.0	977.2
353.15	987.2	1019.1	989.2	973.1
358.15	982.8	1016.2	986.3	969.1
363.15	978.5	1013.3	983.5	965.1

^aStandard uncertainties u are $u(T) = 0.02$ K, $u(p) = 10$ kPa, and the combined expanded uncertainty U_c is $U_c(\rho) = 0.5$ $\text{kg}\cdot\text{m}^{-3}$, with a expanded uncertainty at the 0.95 confidence level ($k \approx 2$).

Supporting Information, depicts the relative deviations between the experimental data obtained in this work and those already reported in literature.^{16–18} Among the ILs studied here, only density data for $[\text{C}_4\text{mim}][\text{CH}_3\text{CO}_2]$ were found. The average relative deviations (for the density data at diverse temperatures) are -0.62% , -0.10% , and 0.21% in respect to the results reported by Bogolitsyn et al.,¹⁶ Tariq et al.,¹⁷ and Xu et al.¹⁸ In general, small deviations are observed among different authors for density data.

To allow a more comprehensive understanding on the effect of the IL cation toward their density values, the results for $[\text{C}_2\text{mim}][\text{CH}_3\text{CO}_2]$ ¹³ are also shown in Figure 2 along with the results gathered in this work. For a given temperature, for instance 320 K, the density of the acetate-based ILs decreases in the following sequence: $[\text{C}_2\text{mim}][\text{CH}_3\text{CO}_2] > [\text{C}_4\text{mim}][\text{CH}_3\text{CO}_2] > [\text{C}_2\text{im}][\text{CH}_3\text{CO}_2] > [\text{C}_4\text{mpyr}][\text{CH}_3\text{CO}_2] > [\text{N}_{0112}][\text{CH}_3\text{CO}_2]$. From the obtained results, the ammonium-based fluid is the less dense. On the other hand, the increase of

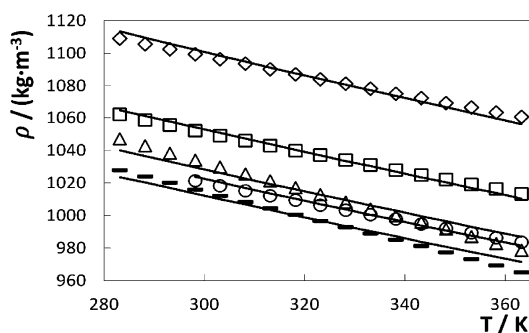


Figure 2. Experimental density data (symbols) as a function of temperature and respective prediction using the Gardas and Coutinho group contribution method²¹ (lines) for the ILs: \diamond , $[\text{C}_2\text{mim}][\text{CH}_3\text{CO}_2]$ ¹³; \square , $[\text{C}_4\text{mim}][\text{CH}_3\text{CO}_2]$; \triangle , $[\text{C}_2\text{im}][\text{CH}_3\text{CO}_2]$; \circ , $[\text{C}_4\text{mpyr}][\text{CH}_3\text{CO}_2]$; $-$, $[\text{N}_{0112}][\text{CH}_3\text{CO}_2]$.

the alkyl side chain length in 1-alkyl-3-methylimidazolium-based fluids leads to a decrease in density. This trend is in agreement with literature data for ILs composed of other anions.^{32–34} In accordance, the protic $[\text{C}_2\text{im}][\text{CH}_3\text{CO}_2]$ IL is more dense than the disubstituted imidazolium-based ILs. Moreover, the pyrrolidinium-based ILs is less dense than its imidazolium-based counterpart (two five-sided rings), as previously observed for ILs constituted by different anions.³⁵

The density data measured in this work were further used to extend the parameter compilation on the group contribution method previously proposed by Gardas and Coutinho.²¹ The ionic volumes for the cations 1-ethyl-imidazolium and N,N -dimethyl- N -ethylammonium were estimated based solely on the density values reported in this work due to the lack of literature data for ILs composed of the same cations, yet with different anions. The new parameters proposed for the ionic volumes are reported in Table 3 along with those previously

Table 3. Ionic Volumes, V , Determined Using the Gardas and Coutinho Group Contribution Model²¹

ionic species		$V/\text{\AA}^3$
	Cation	
$[\text{C}_2\text{im}]^+$		165
$[\text{C}_2\text{mim}]^{+21}$		182
$[\text{C}_4\text{mim}]^{+21}$		238
$[\text{C}_4\text{mpyr}]^{+21}$		253
$[\text{N}_{0112}]^+$		245
	Anion	
$[\text{CH}_3\text{CO}_2]^{-21}$		86
	Additional Groups	
CH_2^{21}		28

reported.²¹ Figure 2 compares the experimental and the predicted density values²¹ as a function of temperature. Predicted values are in close agreement with the experimental data while presenting an average absolute relative deviation of 0.15 % for $[\text{C}_4\text{mim}][\text{CH}_3\text{CO}_2]$, 0.40 % for $[\text{C}_2\text{im}][\text{CH}_3\text{CO}_2]$, 0.14 % for $[\text{C}_4\text{mpyr}][\text{CH}_3\text{CO}_2]$, and 0.27 % for $[\text{N}_{0112}][\text{CH}_3\text{CO}_2]$. Therefore, this method shows to be valuable in the prediction of density data for new ILs whenever experimental data are not available.

The isobaric thermal expansion coefficients, α_p , were calculated through the application of eq 1

$$\alpha_p = -\frac{1}{\rho} \left(\frac{\partial \rho}{\partial T} \right)_p = - \left(\frac{\partial \ln \rho}{\partial T} \right)_p \quad (1)$$

where ρ is the density in $\text{kg}\cdot\text{m}^{-3}$, T is the temperature in K, and p is a fixed pressure.

The α_p values of the studied ionic fluids at 298.15 K are presented in Table 4 and were calculated from the linear relationship between ρ and T . The isobaric thermal expansion

Table 4. Thermal Expansion Coefficients, α_p , for the Studied ILs at 298.15 K

ionic liquid	$10^4 (\alpha_p \pm \sigma^a)/\text{K}^{-1}$
$[\text{C}_2\text{im}][\text{CH}_3\text{CO}_2]$	8.3 ± 0.2
$[\text{C}_4\text{mim}][\text{CH}_3\text{CO}_2]$	5.8 ± 0.1
$[\text{C}_4\text{mpyr}][\text{CH}_3\text{CO}_2]$	5.7 ± 0.1
$[\text{N}_{0112}][\text{CH}_3\text{CO}_2]$	7.7 ± 0.1

^aStandard deviation.

coefficients decrease in the following IL cation sequence: $[\text{C}_2\text{mim}]^+ > [\text{N}_{0112}]^+ > [\text{C}_4\text{mim}]^+ > [\text{C}_4\text{mpyr}]^+ > [\text{C}_2\text{mim}]^+$. From the gathered values, aprotic ILs present lower isobaric thermal expansion values than protic ILs. The α_p values displayed in Table 4 are in good agreement with literature data for $[\text{C}_4\text{mim}][\text{CH}_3\text{CO}_2]$.^{18,36}

Viscosity. The new experimental dynamic viscosity data are presented in Table 5, and the relative deviations between the

Table 5. Experimental Dynamic Viscosity Values, η , at Temperature T , for the Studied ILs at Pressure $p = 0.1 \text{ MPa}$ ^a

T/K	$\eta/(\text{mPa}\cdot\text{s})$			
	$[\text{C}_4\text{mim}][\text{CH}_3\text{CO}_2]$	$[\text{C}_4\text{mpyr}][\text{CH}_3\text{CO}_2]$	$[\text{C}_2\text{mim}][\text{CH}_3\text{CO}_2]$	$[\text{N}_{0112}][\text{CH}_3\text{CO}_2]$
283.15	1037		7.88	26.2
288.15	659		6.67	20.9
293.15	429		5.71	16.4
298.15	297	107	4.95	14.0
303.15	210	79.9	4.34	11.7
308.15	152	61.3	3.83	9.89
313.15	112	48.5	3.39	8.27
318.15	86.1	38.3	3.05	7.32
323.15	66.8	31.1	2.75	6.38
328.15	52.8	25.6	2.49	5.61
333.15	42.7	21.6	2.26	4.87
338.15	34.7	18.1	2.08	4.43
343.15	28.7	15.4	1.91	3.97
348.15	24.0	13.3	1.76	3.58
353.15	20.8	11.9	1.64	3.13
358.15	17.5	10.2	1.52	2.94
363.15	15.1	8.98	1.41	2.69

^aStandard uncertainties u are $u(T) = 0.02 \text{ K}$, $u(p) = 10 \text{ kPa}$, and the combined expanded uncertainty U_c is $U_c(\eta) = 0.35 \%$, with an expanded uncertainty at the 0.95 confidence level ($k \approx 2$).

data collected in this work and those reported in the literature are depicted in Figure S2 provided in the Supporting Information.^{14,19} The viscosity of $[\text{C}_2\text{mim}][\text{CH}_3\text{CO}_2]$ was previously determined by us.¹³ The average relative deviations are -33% when compared with the data published by Crosthwaite et al.¹⁹ and -29% to those published by Fendt et al.¹⁴ When compared with density data, larger differences are observed in the viscosity values obtained by different authors. This property is highly “sensitive” to the presence of impurities or to the adsorption of moisture during the experimental measurements. In addition, the measurement technique, the sample purification steps, and the sample handling are also additional factors that may lead to large divergences in the viscosity values.

Viscosity is the internal resistance of a fluid to a shear stress, and in general, ILs present higher viscosities than conventional molecular solvents. The dynamic viscosity exhibited in Figure 3, for instance at 298.15 K, decreases in the following sequence: $[\text{C}_4\text{mim}][\text{CH}_3\text{CO}_2] > [\text{C}_2\text{mim}][\text{CH}_3\text{CO}_2] > [\text{C}_4\text{mpyr}][\text{CH}_3\text{CO}_2] > [\text{N}_{0112}][\text{CH}_3\text{CO}_2] > [\text{C}_2\text{mim}][\text{CH}_3\text{CO}_2]$. The viscosity data in Figure 3 are plotted as $\ln \eta$ vs $1/T$ for a clearer perception of the data. The viscosity increases with the alkyl side chain length increase in 1-alkyl-3-methylimidazolium acetate ILs. This trend is already well-documented in literature for 1-alkyl-3-methylimidazolium ILs³⁷ and was explained based on the increase on the van der Waals interactions between the

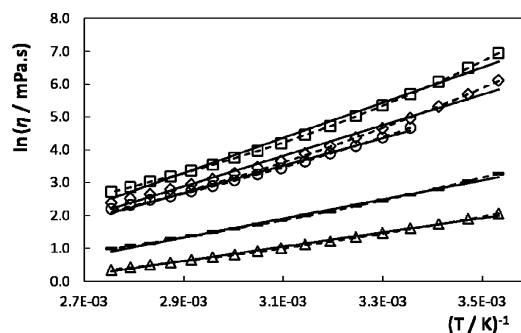


Figure 3. Experimental viscosity data (symbols) as a function of temperature and linear approximations using the Vogel–Tammann–Fulcher equation (dashed lines) and Arrhenius equation (solid lines) for the ILs: \square , $[\text{C}_4\text{mim}][\text{CH}_3\text{CO}_2]$; \diamond , $[\text{C}_2\text{mim}][\text{CH}_3\text{CO}_2]$;¹³ \circ , $[\text{C}_4\text{mpyr}][\text{CH}_3\text{CO}_2]$; \triangle , $[\text{C}_2\text{im}][\text{CH}_3\text{CO}_2]$; ∇ , $[\text{N}_{0211}][\text{CH}_3\text{CO}_2]$.

alkyl side-chains of the cations³⁸ and on the proportion of the charged species in the overall fluid (“ionicity”).³⁹

Noteworthy in the dynamic viscosity data presented in Figure 3 is the dependence on temperature of the acetate-based ILs, which can be divided into two major groups: (i) $[\text{C}_2\text{mim}][\text{CH}_3\text{CO}_2]$, $[\text{C}_4\text{mim}][\text{CH}_3\text{CO}_2]$, and $[\text{C}_4\text{mpyr}][\text{CH}_3\text{CO}_2]$ which show a marked increase on viscosity with a decrease in temperature and (ii) the two protic ILs whereas the increase in viscosity over the temperature range is much less pronounced.

A smooth variation of viscosity with temperature is observed with 1-butyl-3-methylimidazolium-based ILs combined with other anions, such as, for instance, $[\text{NTf}_2]^-$, $[\text{CF}_3\text{SO}_3]^-$, or $[\text{N}(\text{CN})_2]^-$.^{23,37,39} At 298 K, the viscosities of $[\text{C}_2\text{mim}][\text{NTf}_2]$ and $[\text{C}_4\text{mim}][\text{NTf}_2]$ are, respectively, (33.00 and 50.62) mPa·s,³⁷ whereas at the same temperature, the viscosities of $[\text{C}_2\text{mim}][\text{CH}_3\text{CO}_2]$ and $[\text{C}_4\text{mim}][\text{CH}_3\text{CO}_2]$ are much higher being, respectively, (143.61 and 297.39) mPa·s. This marked dependence of viscosity with temperature might be explained by the disruption of hydrogen bonds, which could also explain the high viscosity values observed for the imidazolium-acetate-based ILs at low temperatures. Indeed, molecular dynamics simulations and neutron diffraction studies on 1-ethyl-3-methylimidazolium acetate revealed the liquid structure as in-plane interactions of acetate oxygen atoms with the three imidazolium ring hydrogens and cation–cation planar stacking above/below the imidazolium rings.⁴⁰ This in-plane organized liquid structure through strong directional hydrogen bonds for the imidazolium-based ILs also supports the intriguing observation of a lower value of viscosity for the $[\text{C}_4\text{mpyr}][\text{CH}_3\text{CO}_2]$ as compared with $[\text{C}_4\text{mim}][\text{CH}_3\text{CO}_2]$ —contrary to what has been reported for $[\text{C}_4\text{mpyr}][\text{NTf}_2]$ and $[\text{C}_4\text{mim}][\text{NTf}_2]$.^{39,41} Trying to foster a deeper analysis on this phenomenon, we further carried out mass spectrometry studies. These observations are in fact supported by mass spectrometry data concerning the gas phase fragmentation of isolated $[(\text{Cation})_2\text{Anion}]^+$ aggregates induced by collision with a neutral gas (MS/MS). Further details on the technique can be found elsewhere.⁴² The only fragmentation usually observed is the separation of the neutral IL from the aggregate, which is also the case for $[\text{C}_4\text{mpyr}][\text{CH}_3\text{CO}_2]$. Surprisingly, for $[\text{C}_2\text{mim}][\text{CH}_3\text{CO}_2]$ and $[\text{C}_4\text{mim}][\text{CH}_3\text{CO}_2]$ a competition between the loss of the neutral IL and acetic acid is observed, which indicates a strong interaction between the acetate and one of the hydrogens at the imidazolium ring. Details on the

experimental procedure and results are presented in the Supporting Information.

The two protic ILs display remarkably low viscosities, and this effect is particularly notorious with the [C₂im][CH₃CO₂] which presents viscosities of the same order of magnitude of molecular solvents, such as water. These values are in agreement with previously published values for 1-methylimidazolium acetate.^{15,43} Moreover, as stated above, the viscosity variation of protic ILs with temperature is much less significant than for aprotic ILs, probably due to less prevalent hydrogen bonding. In a study on ionicity and proton transfer in protic ILs, McFarlane et al. also observed these differences in behavior when comparing the viscosity dependence on temperature of primary-amine- vs tertiary-amine-based ILs with the acetate anion.⁴³ Analogously to the results here presented, the tertiary amines show lower viscosities and a weak dependence on temperature.⁴⁴ Together with the analysis of Walden plots, the authors suggested a lack of complete proton transfer or formation of neutral clusters for these amines.⁴⁴ The ionicity of protic ILs has been discussed in terms of the difference between the pK_a^{aq} of the protonated cation and the pK_a^{aq} of the neutral anion.⁴⁵ Measurements of chemical shift differences between ring protons in the methylpyrrolidinium cation (pK_a^{aq}) in a series of ILs show that the methanesulfonate-based fluid (pK_a^{aq}(CH₃SO₃H) ≈ -2) is highly ionized; yet, the acetate-based fluid (pK_a^{aq}(CH₃COOH) = 4.75) is less so.⁴⁵ Assuming that in [C₂im][CH₃CO₂] we are in fact in the presence of a mixture of cations/anions combined with neutral acid/base species, these neutrals could be the major reason behind their low viscosity as compared with [C₂mim][CH₃CO₂]. The viscosity value of 54 mPa·s, reported in the literature⁴⁶ for [C₂im][NTf₂] formed with the super acid (CF₃SO₂)₂NH (pK_a^{aq} ≈ -4), seems to corroborate this hypothesis.

The Vogel–Tammann–Fulcher model usually applied to “glass-forming” liquids, described in eq 2, was used to correlate the experimental dynamic viscosity data of the studied ILs,

$$\ln \eta = A_{\eta} + \frac{B_{\eta}}{(T - T_{0\eta})} \quad (2)$$

where η is the dynamic viscosity in mPa·s, T is the temperature in K, and A_{η} , B_{η} , and $T_{0\eta}$ are adjustable parameters.

The parameters A_{η} , B_{η} , and $T_{0\eta}$ were determined from the fitting of the experimental data and are presented in Table 6.

Table 6. Correlation Parameters (A_{η} , B_{η} , and $T_{0\eta}$) Obtained from Fitting of the Experimental Data Using eq 2

ionic liquid	A_{η}	B_{η}/K	$T_{0\eta}/\text{K}$
[C ₂ im][CH ₃ CO ₂]	-9.39	600	151
[C ₄ mim][CH ₃ CO ₂]	-9.46	935	185
[C ₄ mpyr][CH ₃ CO ₂]	-9.01	765	185
[N ₀₁₁₂][CH ₃ CO ₂]	-9.14	630	169

The fitting of the data against the experimental results is depicted in Figure 3. The average absolute relative deviations between the experimental and the fitting data are 0.74 % for [C₂mim][CH₃CO₂], 2.1 % for [C₂im][CH₃CO₂], 0.43 % for [C₄mpyr][CH₃CO₂], and 0.18 % for [N₀₁₁₂][CH₃CO₂].

Albeit the previous Vogel–Tammann–Fulcher equation has been largely used to describe the viscosity of ILs, we also tested the validity of the Arrhenius equation in describing the viscosity data gathered in this work. A common way to analyze the

viscosity–temperature dependence of common fluids is to use the logarithmic form of the Arrhenius equation,^{47,48}

$$\ln \eta = \ln \eta_{\infty} + \frac{E_{\eta}}{RT} \quad (3)$$

where η is the dynamic viscosity, T is the temperature in K, R is the gas universal constant (8.314472 J·K⁻¹·mol⁻¹), η_{∞} is the viscosity at infinite temperature, and E_{η} is the activation energy (J·mol⁻¹) which gives an evaluation of the level of energy required by the ions to move freely inside the IL. E_{η} and η_{∞} were calculated, respectively, from the slope and intercept of the linear representation of eq 3, and their values are presented in Table 7.

Table 7. Activation Energies for (E_{η}) and Infinite Temperature Viscosities (η_{∞}) Obtained from Fitting of the Experimental Data Using Eq 3 and Respective Correlation Coefficients (R^2)

ionic liquid	$E_{\eta} \pm \sigma^a$	$10^4(\eta_{\infty} \pm \sigma^a)$	R^2
	kJ·mol ⁻¹	mPa·s	
[C ₂ mim][CH ₃ CO ₂] ¹³	38.9 ± 1.1	0.23 ± 0.10	0.997
[C ₄ mim][CH ₃ CO ₂]	44.4 ± 1.1	0.05 ± 0.02	0.990
[C ₂ im][CH ₃ CO ₂]	18.2 ± 0.3	33.06 ± 3.44	0.997
[C ₄ mpyr][CH ₃ CO ₂]	33.9 ± 0.7	1.10 ± 0.29	0.995
[N ₀₁₁₂][CH ₃ CO ₂]	24.0 ± 0.4	8.80 ± 1.44	0.995

^aStandard deviation.

The application of eq 3 to fit the experimental data is depicted in Figure 3. In general, good correlation coefficients were obtained ($R^2 \geq 0.99$). However, a close look at the results shows that all data display a concave dependence. This nonlinear $\ln \eta$ vs $1/T$ dependence has been verified for several ILs, including [C₂mim][CH₃CO₂] and [C₄mim][CH₃CO₂].^{47,49,50} Despite the fact that the fitting is not exactly linear, the activation energy and the viscosity at infinite temperature were calculated as a first approximation to characterize all ILs and compare with literature data.⁴⁷ E_{η} is the energy barrier which must be overcome to the ions to move past each other in the ionic fluid. The higher the E_{η} value is, the more difficult it is for the ions to move past each other, and this can be a direct consequence of the size or entanglement of the ions and/or by the presence of stronger interactions in the fluid. At infinite temperature, the interactions which contribute to the viscosity are no longer effective, and thus it is governed purely by the geometric structure of the ions. Therefore, the η_{∞} value describes the structural contribution of the ions to the dynamic viscosity. From the inspection of Table 7, it is clear that protic ILs display lower activation energies, which is a direct result of their structure and lower symmetry. On the other hand, an increase in the cation side alkyl chain length leads to an increase on the activation energy of the IL. Both of these patterns can also be explained by the increased molar mass in the cation that may inhibit the laminar flow. Finally, the pyrrolidinium-based IL displays lower activation energy when compared to the imidazolium-based counterpart, and that could be related with its nonaromatic character. The activation energy of [C₄mim][CH₃CO₂] (44.45 kJ·mol⁻¹) is on the same order of magnitude of [C₄mim][PF₆] (23.94 kJ·mol⁻¹),⁴⁷ although it is significantly higher. This difference is a direct result of the stronger interactions occurring in the IL containing the acetate anion (with improved hydrogen-bonding acceptor ability). In

general, the viscosity at infinite temperature decreases with the increase on the activation energy, and as previously noted by Okoturo and VanderNoot,⁴⁷ meaning that the structural contribution of each ion to the dynamic viscosity cannot be discarded.

Refractive Index. Experimental refractive index data for the studied compounds are presented in Table 8. Although

Table 8. Experimental Refractive Index Values, n_D , at Temperature T , for the Studied ILs at Pressure $p = 0.1 \text{ MPa}$ ^a

T/K	n_D				
	$[\text{C}_2\text{im}][\text{CH}_3\text{CO}_2]$	$[\text{C}_2\text{mim}][\text{CH}_3\text{CO}_2]$	$[\text{C}_4\text{mim}][\text{CH}_3\text{CO}_2]$	$[\text{C}_4\text{mpyr}][\text{CH}_3\text{CO}_2]$	$[\text{N}_{0112}][\text{CH}_3\text{CO}_2]$
283.15	1.46347	1.50402	1.49269	1.47263	1.42303
288.15	1.46160	1.50267	1.49158	1.47144	1.42143
293.15	1.45966	1.50129	1.49021	1.47075	1.41983
298.15	1.45769	1.49992	1.48890	1.46998	1.41819
303.15	1.45576	1.49854	1.48725	1.46868	1.41655
308.15	1.45379	1.49718	1.48580	1.46736	1.41492
313.15	1.45185	1.49581	1.48438	1.46603	1.41328
318.15	1.44985	1.49447	1.48297	1.46461	1.41156
323.15	1.44791	1.49307	1.48060	1.46320	1.40991
328.15	1.44593	1.49171	1.47915	1.46178	1.40820
333.15	1.44395	1.49035	1.47770	1.46042	1.40649
338.15	1.44197	1.48899	1.47624	1.45900	1.40476
343.15	1.44000	1.48756	1.47463	1.45755	1.40312
348.15	1.43800	1.48613	1.47318	1.45619	1.40138
353.15	1.43607	1.48476	1.47180	1.45479	1.39963

^aStandard uncertainties u are $u(T) = 0.01 \text{ K}$, $u(p) = 10 \text{ kPa}$, and the combined expanded uncertainty U_c is $U_c(n_D) = 2 \cdot 10^{-5}$, with a expanded uncertainty at the 0.95 confidence level ($k \approx 2$).

$[\text{C}_4\text{mpyr}][\text{CH}_3\text{CO}_2]$ is solid at room temperature, the refractive indices at lower temperatures were also measured in the supercooled liquid. The refractive index values for the $[\text{CH}_3\text{CO}_2]$ -based ILs decrease in the following cationic sequence: $[\text{C}_2\text{mim}]^+ > [\text{C}_4\text{mim}]^+ > [\text{C}_4\text{mpyr}]^+ > [\text{N}_{0112}]^+ > [\text{C}_2\text{im}]^+$.

Refractive index data for acetate-based ILs are scarce in literature. Figure S2, provided in the Supporting Information, presents the percentage relative deviations between our data and those from literature. For $[\text{C}_2\text{mim}][\text{CH}_3\text{CO}_2]$ the relative deviations are -0.064% ¹³ and 0.056% ,²⁰ respectively, while for $[\text{C}_4\text{mim}][\text{CH}_3\text{CO}_2]$ ¹⁶ the relative deviation is -30% . $[\text{C}_2\text{mim}][\text{CH}_3\text{CO}_2]$ was previously measured by us,¹³ using a distinct equipment. In general, a good agreement is observed between different sets of results.

The prediction of the refractive index for the ILs studied was also accomplished with the group contribution method proposed by Gardas and Coutinho,²² which are depicted in Figure 4, and that follows a linear function of the form,

$$n_D = A_{n_D} - B_{n_D} T \quad (4)$$

where

$$A_{n_D} = \sum_{i=1}^k n_i a_{i,n_D} \quad (5)$$

$$B_{n_D} = \sum_{i=1}^k n_i b_{i,n_D} \quad (6)$$

where n_i is the number of group of type i , and k is the total number of different groups in the molecule.

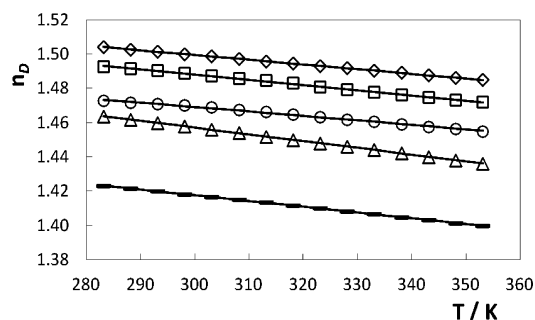


Figure 4. Experimental refractive index data (symbols) as a function of temperature and respective prediction using the group contribution method proposed by Gardas and Coutinho²² (lines): \diamond , $[\text{C}_2\text{mim}][\text{CH}_3\text{CO}_2]$; \square , $[\text{C}_4\text{mim}][\text{CH}_3\text{CO}_2]$; \triangle , $[\text{C}_2\text{im}][\text{CH}_3\text{CO}_2]$; \circ , $[\text{C}_4\text{mpyr}][\text{CH}_3\text{CO}_2]$; $-$, $[\text{N}_{0211}][\text{CH}_3\text{CO}_2]$.

The estimated parameter a_{i,n_D} and b_{i,n_D} for the studied ILs are given in Table 9. New values for a_{i,n_D} and b_{i,n_D} for the ions

Table 9. Group Contribution Parameters (a_{i,n_D} and b_{i,n_D}) of the Group Contribution Method of Gardas and Coutinho²²

ionic species	a_{i,n_D}	$b_{i,n_D}/\text{K}^{-1}$
Cation		
$[\text{C}_2\text{im}]^+$	1.4361	$3.3596 \cdot 10^{-4}$
$[\text{C}_2\text{mim}]^{+22}$	1.4789	$3.0010 \cdot 10^{-4}$
$[\text{C}_4\text{mim}]^{+22}$	1.4876	$3.0927 \cdot 10^{-4}$
$[\text{C}_4\text{mpyr}]^+$	1.4080	$2.0212 \cdot 10^{-4}$
$[\text{N}_{0112}]^+$	1.3792	$2.7764 \cdot 10^{-4}$
Anion		
$[\text{CH}_3\text{CO}_2]^{-13}$	0.1387	$5.661 \cdot 10^{-5}$
Additional Groups		
CH_2^{22}	0.0045	$4.587 \cdot 10^{-6}$
CH_3^{22}	0.0353	$7.330 \cdot 10^{-5}$

$[\text{C}_4\text{mpyr}]^+$, $[\text{C}_2\text{im}]^+$, and $[\text{N}_{0112}]^+$ are presented and were estimated with the data gathered in this work. The average absolute relative deviation between the experimental and the fitting data are 0.0018 % for $[\text{C}_2\text{mim}][\text{CH}_3\text{CO}_2]$, 0.017 % for $[\text{C}_4\text{mim}][\text{CH}_3\text{CO}_2]$, 0.0079 % for $[\text{C}_2\text{im}][\text{CH}_3\text{CO}_2]$, 0.024 % for $[\text{C}_4\text{mpyr}][\text{CH}_3\text{CO}_2]$, and 0.0082 % for $[\text{N}_{0112}][\text{CH}_3\text{CO}_2]$.

Surface Tension. The surface tension values for the $[\text{CH}_3\text{CO}_2]$ -based ILs are presented in Table 10. In literature, surface tension values of $[\text{CH}_3\text{CO}_2]$ -based ILs are scarce.⁵¹ Besides the data for $[\text{C}_2\text{mim}][\text{CH}_3\text{CO}_2]$ previously reported by us,²⁹ only surface tension values for $[\text{C}_4\text{mim}][\text{CH}_3\text{CO}_2]$ were found.¹⁸ The average relative deviation between the data collected in this work and those reported is -7.9% .¹⁸ The relative deviations as a function of temperature are depicted in Figure S2 provided in the Supporting Information.

The experimental surface tension values show that the IL cation plays a significant role in the structural organization of the IL at the air–liquid interface as shown in Table 10. Previously we have reported surface tension data for $[\text{C}_2\text{mim}][\text{CH}_3\text{CO}_2]$,²⁹ and compared with the results obtained here, at 298 K the surface tension decreases in the following sequence: $[\text{C}_2\text{mim}][\text{CH}_3\text{CO}_2] > [\text{C}_2\text{im}][\text{CH}_3\text{CO}_2] > [\text{C}_4\text{mpyr}][\text{CH}_3\text{CO}_2] > [\text{C}_4\text{mim}][\text{CH}_3\text{CO}_2] > [\text{N}_{0112}][\text{CH}_3\text{CO}_2]$. Among the studied ILs, the ammonium-based IL presents the lower values of surface tension. For the 1-alkyl-3-methylimidazolium-based fluids, an increase of the alkyl chain length leads

Table 10. Experimental Surface Tension, γ , at Temperature T , for the Studied ILs at Pressure $p = 0.1 \text{ MPa}^a$

[C ₂ im][CH ₃ CO ₂]		[C ₄ mim][CH ₃ CO ₂]		[C ₄ mpyr][CH ₃ CO ₂]		[N ₀₂₁₁][CH ₃ CO ₂]	
T/K	$\gamma/(\text{mN}\cdot\text{m}^{-1})$	T/K	$\gamma/(\text{mN}\cdot\text{m}^{-1})$	T/K	$\gamma/(\text{mN}\cdot\text{m}^{-1})$	T/K	$\gamma/(\text{mN}\cdot\text{m}^{-1})$
298.1	37.8	298.0	36.4	298.3	37.4	298.2	33.5
307.8	36.7	307.8	35.9	307.9	36.8	308.1	32.7
318.5	36.1	318.0	35.5	318.0	36.4	318.0	32.1
328.3	35.0	328.6	35.1	328.4	36.1	328.4	31.3
339.9	33.7	339.0	34.7	338.5	35.6	338.2	30.5
344.2	33.3	343.5	34.4	343.0	35.4		

^aStandard uncertainties u are $u(T) = 0.1 \text{ K}$, $u(p) = 10 \text{ kPa}$, and the combined expanded uncertainty U_c is $U_c(\gamma) = 0.1 \text{ mN}\cdot\text{m}^{-1}$, with a expanded uncertainty at the 0.95 confidence level ($k \approx 2$).

Table 11. Surface Thermodynamic Functions of the Studied ILs and Estimated Critical Temperatures, Using Both the Empirical Equations of Eötvös ($(T_c)_{\text{Eot}}$)⁶⁰ and Guggenheim ($(T_c)_{\text{Gug}}$)⁶¹

ionic liquid	$(S^\gamma \pm \sigma^a) \cdot 10^{-5}$	$(H^\gamma \pm \sigma^a) \cdot 10^{-2}$	$(T_c)_{\text{Eot}}$	$(T_c)_{\text{Gug}}$
	$\text{J}\cdot\text{m}^{-2}\cdot\text{K}^{-1}$	$\text{J}\cdot\text{m}^{-2}$	K	K
[C ₂ im][CH ₃ CO ₂]	9.6 ± 0.5	6.6 ± 0.1	793 ± 2	775.8 ± 0.8
[C ₄ mim][CH ₃ CO ₂]	4.2 ± 0.1	4.88 ± 0.04	1582 ± 5	1353.5 ± 0.8
[C ₄ mpyr][CH ₃ CO ₂]	4.3 ± 0.2	5.01 ± 0.08	1585 ± 9	1357.1 ± 0.8
[N ₀₂₁₁][CH ₃ CO ₂]	7.4 ± 0.3	5.57 ± 0.08	872 ± 2	844.2 ± 0.8

^aStandard deviation.

to a decrease on the surface tension. This trend is in agreement with previous surface tension data for other 1-alkyl-3-methylimidazolium ILs.⁵² However, the exclusion of a $-\text{CH}_3$ group in [C₂mim]⁺ to gives [C₂im]⁺ leads to a decrease in the surface tension. This trend was previously observed by Freire et al.⁵³ with the exclusion of a $-\text{CH}_3$ group from the most acidic hydrogen at the imidazolium ring, although only verified with aprotic ILs. Outstandingly, the substitution of an alkyl group by an hydrogen seems to have an important impact in what concerns the surface tension dependence on temperature. Moreover, the pyrrolidinium-based IL presents higher surface tensions values than its imidazolium-based counterpart, which is in agreement with literature data for other anions.⁵⁴

The surface thermodynamic properties, namely, the surface entropy and the surface enthalpy, were derived using the quasi-linear dependence of the surface tension with temperature. The surface entropy, S^γ , can be calculated according to the following equation^{55,56}

$$S^\gamma = -\left(\frac{d\gamma}{dT}\right) \quad (7)$$

while the surface enthalpy, H^γ , according to^{55,56}

$$H^\gamma = \gamma - T\left(\frac{d\gamma}{dT}\right) \quad (8)$$

where γ stands for the surface tension and T for the temperature.

The values of the thermodynamic functions of all of the ILs investigated, with the respective standard deviations,⁵⁷ are presented in Table 11.

In agreement with results previously reported for other ILs,^{52–54} this class of fluids exhibits remarkably low surface entropy when compared with molecular organic compounds. These results indicate a high surface organization, as well as a highly structured liquid phase in ILs. Lower surface entropies are observed for [C₂mim][CH₃CO₂], [C₄mim][CH₃CO₂], and [C₄mpyr][CH₃CO₂]. On the other hand, the protic ILs, [C₂im][CH₃CO₂] and [N₀₁₁₂][CH₃CO₂], display higher sur-

face entropies suggesting a less structured liquid phase and in agreement with their lower ionic character discussed above.^{39,44–46}

The critical temperature of fluids is a recurrent property commonly used in corresponding state relationships involving equilibrium and transport properties.⁵⁸ However, the determination of the critical temperatures of ILs is a challenging task since they decompose before reaching those high temperatures. Rebelo et al.⁵⁹ proposed the use of the Eötvös⁶⁰ and Guggenheim⁶¹ equations to estimate the hypothetical critical temperature of ILs, and they are described accordingly,

$$\gamma\left(\frac{M}{\rho}\right)^{2/3} = K(T_c - T) \quad (9)$$

$$\gamma = K\left(1 - \frac{T}{T_c}\right)^{11/9} \quad (10)$$

where T_c is the critical temperature, M is the molecular weight, ρ is the density, and K is a fitted parameter.

The critical temperature values estimated from the surface tension data are reported in Table 11. By analyzing the critical temperatures a significant difference between aprotic and protic ILs can be observed. Protic ILs present significantly lower critical temperatures. For instance, the exclusion of a $-\text{CH}_3$ group in [C₂mim]⁺, to give [C₂im]⁺, leads to a considerable decrease in the critical temperature.

CONCLUSIONS

Acetate-based ILs have been explored in the past few years due to their unique properties. Acetate-based fluids have shown great promise in the CO₂ capture and dissolution of biomass and lignocellulosic materials. Five acetate-based ILs were here characterized, and new experimental data on density, viscosity, refractive index, and surface tension were reported. From the temperature dependence of the several properties, additional parameters, such as the isobaric thermal expansion coefficient, the surface thermodynamics properties, and critical temperature

of all ILs were further estimated and presented. The group contribution methods proposed by Gardas and Coutinho were also evaluated and used to predict the density and refractive index of the investigated ILs. New group parameters for chemical groups not previously available were proposed.

■ ASSOCIATED CONTENT

● Supporting Information

Thermogravimetric analysis and electrospray ionization tandem mass spectra details. This material is available free of charge via the Internet at <http://pubs.acs.org>.

■ AUTHOR INFORMATION

Corresponding Author

*Tel.: +351-234-370200. Fax: +351-234-370084. E-mail address: maragfreire@ua.pt.

Funding

This work was funded by QREN SI-I&DT Project No. 11551 from UE/FEDER through COMPETE program. The authors also acknowledge FCT—Fundação para a Ciência e a Tecnologia for the projects Pest-C/CTM/LA0011/2011 and PTDC/EQU-FTT/102166/2008 and for the postdoctoral grant (SFRH/BPD/41781/2007) of M.G.F.

Notes

The authors declare no competing financial interest.

■ REFERENCES

- (1) Marsh, K. N.; Boxall, J. A.; Lichtenthaler, R. Room Temperature Ionic Liquids and Their Mixtures - A Review. *Fluid Phase Equilib.* **2004**, *219*, 93–98.
- (2) Chiappe, C.; Pieraccini, D. Ionic liquids: Solvent Properties and Organic Reactivity. *J. Phys. Org. Chem.* **2005**, *18*, 275–297.
- (3) Rogers, R. D.; Seddon, K. R. Ionic liquids - Solvents of the Future? *Science* **2003**, *302*, 792–793.
- (4) Shillett, M. B.; Drew, D. W.; Cantini, R. A.; Yokozeki, A. Carbon Dioxide Capture Using Ionic Liquid 1-Butyl-3-methylimidazolium Acetate. *Energy Fuels* **2010**, *24*, 5781–5789.
- (5) Janiczek, P.; Kalb, R. S.; Thonhauser, G.; Gamse, T. Carbon Dioxide Absorption in a Technical-Scale-Plant utilizing an Imidazolium Based Ionic Liquid. *Sep. Purif. Technol.* **2012**, 10.1016/j.seppur.2012.03.003.
- (6) Mattedi, S.; Carvalho, P. J.; Coutinho, J. A. P.; Alvarez, V. H.; Iglesias, M. High pressure CO₂ solubility in N-methyl-2-hydroxyethylammonium Protic Ionic Liquids. *J. Supercrit. Fluids* **2011**, *56*, 224–230.
- (7) Carvalho, P. J.; Álvarez, V. C. H.; Schröder, B.; Gil, A. M.; Marrucho, I. M.; Aznar, M. N.; Santos, L. s. M. N. B. F.; Coutinho, J. A. P. Specific Solvation Interactions of CO₂ on Acetate and Trifluoroacetate Imidazolium Based Ionic Liquids at High Pressures. *J. Phys. Chem. B* **2009**, *113*, 6803–6812.
- (8) Shill, K.; Padmanabhan, S.; Xin, Q.; Prausnitz, J. M.; Clark, D. S.; Blanch, H. W. Ionic Liquid Pretreatment of Cellulosic Biomass: Enzymatic Hydrolysis and Ionic Liquid Recycle. *Biotechnol. Bioeng.* **2011**, *108*, 511–520.
- (9) Sant'ana da Silva, A.; Lee, S. H.; Endo, T.; Bon, E. P. Major Improvement in the Rate and Yield of Enzymatic Saccharification of Sugarcane Bagasse via Pretreatment with the Ionic Liquid 1-ethyl-3-methylimidazolium Acetate ([Emim][Ac]). *Bioresour. Technol.* **2011**, *102*, 10505–10509.
- (10) Fu, D.; Mazza, G.; Tamaki, Y. Lignin Extraction from Straw by Ionic Liquids and Enzymatic Hydrolysis of the Cellulosic Residues. *J. Agric. Food Chem.* **2010**, *58*, 2915–2922.
- (11) Freire, M. G.; Teles, A. R. R.; Ferreira, R. A. S.; Carlos, L. D.; Lopes-da-Silva, J. A.; Coutinho, J. A. P. Electrospun Nanosized Cellulose Fibers using Ionic Liquids at Room Temperature. *Green Chem.* **2011**, *13*, 3173–3180.
- (12) Remsing, R. C.; Swatloski, R. P.; Rogers, R. D.; Moyna, G. Mechanism of Cellulose Dissolution in the Ionic Liquid 1-n-butyl-3-methylimidazolium Chloride: a ¹³C and ^{35/37}Cl NMR Relaxation Study on Model Systems. *Chem. Commun.* **2006**, 1271–1273.
- (13) Freire, M. G.; Teles, A. R. R.; Rocha, M. A. A.; Schröder, B.; Neves, C. M. S. S.; Carvalho, P. J.; Evtuguin, D. V.; Santos, L. M. N. B. F.; Coutinho, J. A. P. Thermophysical Characterization of Ionic Liquids Able To Dissolve Biomass. *J. Chem. Eng. Data* **2011**, *56*, 4813–4822.
- (14) Fendt, S.; Padmanabhan, S.; Blanch, H. W.; Prausnitz, J. M. Viscosities of Acetate or Chloride-Based Ionic Liquids and Some of Their Mixtures with Water or Other Common Solvents. *J. Chem. Eng. Data* **2011**, *56*, 31–34.
- (15) Qian, W.; Xu, Y.; Zhu, H.; Yu, C. Properties of Pure 1-methylimidazolium Acetate Ionic Liquid and its Binary Mixtures with Alcohols. *J. Chem. Thermodyn.* **2012**, *49*, 87–94.
- (16) Bogolitsyn, K. G.; Skrebets, T. E.; Makhova, T. A. Physicochemical Properties of 1-butyl-3-methylimidazolium Acetate. *Russ. J. Gen. Chem.* **2009**, *79*, 125–128.
- (17) Tariq, M.; Forte, P. A. S.; Gomes, M. F. C.; Lopes, J. N. C.; Rebelo, L. P. N. Densities and refractive indices of imidazolium- and phosphonium-based ionic liquids: Effect of temperature, alkyl chain length, and anion. *J. Chem. Thermodyn.* **2009**, *41*, 790–798.
- (18) Xu, A.; Wang, J.; Zhang, Y.; Chen, Q. Effect of Alkyl Chain Length in Anions on Thermodynamic and Surface Properties of 1-Butyl-3-methylimidazolium Carboxylate Ionic Liquids. *Ind. Eng. Chem. Res.* **2012**, *51*, 3458–3465.
- (19) Crosthwaite, J. M.; Muldoon, M. J.; Dixon, J. K.; Anderson, J. L.; Brennecke, J. F. Phase Transition and Decomposition Temperatures, Heat Capacities and Viscosities of Pyridinium Ionic Liquids. *J. Chem. Thermodyn.* **2005**, *37*, 559–568.
- (20) Fröba, A. P.; Rausch, M. H.; Krzeminski, K.; Assenbaum, D.; Wasserscheid, P.; Leipertz, A. Thermal Conductivity of Ionic Liquids: Measurement and Prediction. *Int. J. Thermophys.* **2010**, *31*, 2059–2077.
- (21) Gardas, R. L.; Coutinho, J. A. P. Extension of the Ye and Shreeve Group Contribution Method for Density Estimation of Ionic Liquids in a Wide Range of Temperatures and Pressures. *Fluid Phase Equilib.* **2008**, *263*, 26–32.
- (22) Gardas, R. L.; Coutinho, J. A. P. Group Contribution Methods for the Prediction of Thermophysical and Transport Properties of Ionic Liquids. *AIChE J.* **2009**, *55*, 1274–1290.
- (23) Carvalho, P. J.; Regueira, T.; Santos, L.; Fernandez, J.; Coutinho, J. A. P. Effect of Water on the Viscosities and Densities of 1-Butyl-3-methylimidazolium Dicyanamide and 1-Butyl-3-methylimidazolium Tricyanomethane at Atmospheric Pressure. *J. Chem. Eng. Data* **2010**, *55*, 645–652.
- (24) Neves, C. M. S. S.; Batista, M. L. S.; Claudio, A. F. M.; Santos, L. M. N. B. F.; Marrucho, I. M.; Freire, M. G.; Coutinho, J. A. P. Thermophysical Properties and Water Saturation of [PF₆]-Based Ionic Liquids. *J. Chem. Eng. Data* **2010**, *55*, S065–S073.
- (25) Oliveira, F. S.; Freire, M. G.; Carvalho, P. J.; Coutinho, J. A. P.; Canongia Lopes, J. N.; Rebelo, L. P. N.; Marrucho, I. M. Structural and Positional Isomerism Influence in the Physical Properties of Pyridinium NTf₂-Based Ionic Liquids: Pure and Water-Saturated Mixtures. *J. Chem. Eng. Data* **2010**, *55*, 4514–4520.
- (26) Viscosity of thermal conductivity of heavy water substance. In *International Association for the Properties of Water Steam: in Physical Chemistry of Aqueous Systems, Proceedings of the 12th International Conference on the Properties of Water and Steam, Orlando, FL, 1994*.
- (27) Jasper, J. J.; Kring, E. V. The Isobaric Surface Tensions and Thermodynamic Properties of the Surfaces of a Series of n-Alkanes, C₅ to C₁₈, 1-Alkenes, C₆ to C₁₆, and of n-Decylcyclopentane, n-Decylcyclohexane and n-Decylbenzene. *J. Phys. Chem.* **1955**, *59*, 1019–1021.
- (28) Somayajulu, G. R. A Generalized Equation for Surface Tension from the Triple Point to the Critical Point. *Int. J. Thermophys.* **1988**, *9*, 559–566.

- (29) Almeida, H. F. D.; Teles, A. R. R.; Lopes-da-Silva, J. A.; Freire, M. G.; Coutinho, J. A. P. Influence of the Anion on the Surface Tension of 1-ethyl-3-methylimidazolium-based Ionic Liquids. *J. Chem. Thermodyn.* **2012**, *54*, 49–54.
- (30) Seeberger, A.; Andresen, A.-K.; Jess, A. Prediction of Long-term Stability of Ionic Liquids at Elevated Temperatures by Means of Non-Isenthalpic Thermogravimetric Analysis. *Phys. Chem. Chem. Phys.* **2009**, *11*, 9375–9381.
- (31) Kamavaram, V.; Reddy, R. G. Thermal Stabilities of Di-alkylimidazolium Chloride Ionic Liquids. *Int. J. Therm. Sci.* **2008**, *47*, 773–777.
- (32) Gardas, R. L.; Freire, M. G.; Carvalho, P. J.; Marrucho, I. M.; Fonseca, I. M. A.; Ferreira, A. G. M.; Coutinho, J. A. P. ρ T Measurements of Imidazolium-Based Ionic Liquids. *J. Chem. Eng. Data* **2007**, *52*, 1881–1888.
- (33) Esperança, J. M. S. S.; Visak, Z. P.; Plechkova, N. V.; Seddon, K. R.; Guedes, H. J. R.; Rebelo, L. P. N. Density, Speed of Sound, and Derived Thermodynamic Properties of Ionic Liquids over an Extended Pressure Range. 4. $[\text{C}_3\text{mim}][\text{NTf}_2]$ and $[\text{C}_5\text{mim}][\text{NTf}_2]$. *J. Chem. Eng. Data* **2006**, *51*, 2009–2015.
- (34) Esperança, J. M. S. S.; Guedes, H. J. R.; Lopes, J. N. C.; Rebelo, L. P. N. Pressure–Density–Temperature (p – ρ – T) Surface of $[\text{C}_6\text{mim}][\text{NTf}_2]$. *J. Chem. Eng. Data* **2008**, *53*, 867–870.
- (35) Gardas, R. L.; Costa, H. F.; Freire, M. G.; Carvalho, P. J.; Marrucho, I. M.; Fonseca, I. M. A.; Ferreira, A. G. M.; Coutinho, J. A. P. Densities and Derived Thermodynamic Properties of Imidazolium-, Pyridinium-, Pyrrolidinium-, and Piperidinium-Based Ionic Liquids. *J. Chem. Eng. Data* **2008**, *53*, 805–811.
- (36) Bogolitsyn, K. G.; Makhova, T. A.; Skrebets, T. E. Application of the Interstice Model to Structure Characterization of 1-butyl-3-methylimidazolium Acetate. *Russ. J. Gen. Chem.* **2010**, *80*, 1355–1357.
- (37) Tariq, M.; Carvalho, P. J.; Coutinho, J. A. P.; Marrucho, I. M.; Canongia Lopes, J. N.; Rebelo, L. P. N. Viscosity of (C2–C14) 1-alkyl-3-methylimidazolium bis(trifluoromethylsulfonyl)amide Ionic Liquids in an Extended Temperature Range. *Fluid Phase Equilib.* **2011**, *301*, 22–32.
- (38) Bonhôte, P.; Dias, A.-P.; Papageorgiou, N.; Kalyanasundaram, K.; Grätzel, M. Hydrophobic, Highly Conductive Ambient-Temperature Molten Salts. *Inorg. Chem.* **1996**, *35*, 1168–1178.
- (39) Tokuda, H.; Tsuzuki, S.; Susan, M. A. B. H.; Hayamizu, K.; Watanabe, M. How Ionic Are Room-Temperature Ionic Liquids? An Indicator of the Physicochemical Properties. *J. Phys. Chem. B* **2006**, *110*, 19593–19600.
- (40) Bowron, D. T.; D’Agostino, C.; Gladden, L. F.; Hardacre, C.; Holbrey, J. D.; Lagunas, M. C.; McGregor, J.; Mantle, M. D.; Mullan, C. L.; Youngs, T. G. A. Structure and Dynamics of 1-Ethyl-3-methylimidazolium Acetate via Molecular Dynamics and Neutron Diffraction. *J. Phys. Chem. B* **2010**, *114*, 7760–7768.
- (41) Bernard, U. L.; Izgorodina, E. I.; MacFarlane, D. R. New Insights into the Relationship between Ion-Pair Binding Energy and Thermodynamic and Transport Properties of Ionic Liquids. *J. Phys. Chem. C* **2010**, *114*, 20472–20478.
- (42) Fernandes, A. M.; Rocha, M. A. A.; Freire, M. G.; Marrucho, I. M.; Coutinho, J. A. P.; Santos, L. M. N. B. F. Evaluation of Cation–Anion Interaction Strength in Ionic Liquids. *J. Phys. Chem. B* **2011**, *115*, 4033–4041.
- (43) MacFarlane, D. R.; Pringle, J. M.; Johansson, K. M.; Forsyth, S. A.; Forsyth, M. Lewis Base Ionic Liquids. *Chem. Commun.* **2006**, 1905–1917.
- (44) Stoimenovski, J.; Izgorodina, E. I.; MacFarlane, D. R. Ionicity and Proton Transfer in Protic Ionic Liquids. *Phys. Chem. Chem. Phys.* **2010**, *12*, 10341–10347.
- (45) Angell, C. A.; Byrne, N.; Belieres, J.-P. Parallel Developments in Aprotic and Protic Ionic Liquids: Physical Chemistry and Applications. *Acc. Chem. Res.* **2007**, *40*, 1228–1236.
- (46) Greaves, T. L.; Drummond, C. J. Protic Ionic Liquids: Properties and Applications. *Chem. Rev.* **2008**, *108*, 206–237.
- (47) Okoturo, O. O.; VanderNoot, T. J. Temperature Dependence of Viscosity for Room Temperature Ionic Liquids. *J. Electroanal. Chem.* **2004**, *568*, 167–181.
- (48) Galán Sánchez, L. M.; Meindersma, G. W.; de Haan, A. B. Solvent Properties of Functionalized Ionic Liquids for CO_2 Absorption. *Chem. Eng. Res. Des.* **2007**, *85*, 31–39.
- (49) Gericke, M.; Schlufner, K.; Liebert, T.; Heinze, T.; Budtova, T. Rheological Properties of Cellulose/Ionic Liquid Solutions: From Dilute to Concentrated States. *Biomacromolecules* **2009**, *10*, 1188–1194.
- (50) Sescousse, R.; Le, K. A.; Ries, M. E.; Budtova, T. Viscosity of Cellulose–Imidazolium-Based Ionic Liquid Solutions. *J. Phys. Chem. B* **2010**, *114*, 7222–7228.
- (51) Tariq, M.; Freire, M. G.; Saramago, B.; Coutinho, J. A. P.; Canongia Lopes, J. N.; Rebelo, L. P. N. Surface Tension of Ionic Liquids and Ionic Liquid Solutions. *Chem. Soc. Rev.* **2012**, *41*, 829–868.
- (52) Carvalho, P. J.; Freire, M. G.; Marrucho, I. M.; Queimada, A. J.; Coutinho, J. A. P. Surface Tensions for the 1-Alkyl-3-methylimidazolium bis(trifluoromethylsulfonyl)imide Ionic Liquids. *J. Chem. Eng. Data* **2008**, *53*, 1346–1350.
- (53) Freire, M. G.; Carvalho, P. J.; Fernandes, A. M.; Marrucho, I. M.; Queimada, A. J.; Coutinho, J. A. P. Surface Tensions of Imidazolium Based Ionic Liquids: Anion, Cation, Temperature and Water Effect. *J. Colloid Interface Sci.* **2007**, *314*, 621–630.
- (54) Carvalho, P. J.; Neves, C. M. S. S.; Coutinho, J. A. P. Surface Tensions of Bis(trifluoromethylsulfonyl)imide Anion-Based Ionic Liquids. *J. Chem. Eng. Data* **2010**, *55*, 3807–3812.
- (55) Adamson, A. W.; Gast, A. P. *Physical chemistry of surfaces*; John Wiley: New York, 1997.
- (56) McNaught, A. D.; Wilkinson, A. *Compendium of Chemical Terminology, IUPAC Recommendations*; Blackwell Science: Cambridge, U.K., 1997.
- (57) Miller, J. C.; Miller, J. N. *Statistics for Analytical Chemistry*; PTR Prentice Hall: Chichester, NY, 1993.
- (58) Poling, B. E.; Prausnitz, J. M.; O’Connell, J. P. *The Properties of Gases and Liquids*; McGraw-Hill: New York, 2001.
- (59) Rebelo, L. P. N.; Canongia Lopes, J. N.; Esperança, J. M. S. S.; Filipe, E. On the Critical Temperature, Normal Boiling Point, and Vapor Pressure of Ionic Liquids. *J. Phys. Chem. B* **2005**, *109*, 6040–6043.
- (60) Shereshefsky, J. L. Surface Tension of Saturated Vapors and the Equation of Eotvos. *J. Phys. Chem.* **1931**, *35*, 1712–1720.
- (61) Guggenheim, E. A. The Principle of Corresponding States. *J. Chem. Phys.* **1945**, *13*, 253–261.